J. Fluid Mech. (1982), *vol.* 123, *pp.* 303–313
Printed in Great Britain

Flow separation in a rotating annulus with bottom topography

By M. A. PAGE

School of Mathematics and Physics, University of East Anglia, Norwich NR4 7TJ, England

(Received 4 March 1982)

The flow in a rotating annular cylinder, of finite depth, is examined when the Rossby number Ro is $O(E^{\frac{1}{2}})$, where E is the Ekman number, and when there is a topography of height $O(E^{\frac{1}{2}})$ on the base of the container. The flow, relative to the rigid axial rotation, is forced by differential rotation of the lid and as it moves over the topography the streamlines are deflected parallel to the bottom surface. This induces $O(1)$ velocity variations near the axial walls of the annulus to which the boundary layers there, of thickness $O(E^{\frac{1}{4}})$, respond. For sufficiently large values of a parameter $\lambda \propto Ro/E^{\frac{1}{2}}$ the skin friction can vanish within these layers, with some similarities to boundary-layer separation in a non-rotating fluid. In this study the interior flow, with horizontal viscous diffusion neglected, is calculated and used to provide a boundary condition for the $E^{\frac{1}{4}}$ layer flow. Once λ exceeds a finite critical value a singularity is encountered in the boundary layer corresponding to flow separation from the wall. This demonstrates that $E^{\frac{1}{4}}$ layers in a rotating fluid, which for $Ro = 0$ have little direct influence on the interior flow, can modify the gross properties of the flow for non-zero Rossby numbers, a conclusion also reached by Walker & Stewartson (1972) in a different context.

1. Introduction

In this paper the flow of a rotating fluid of finite depth at low Rossby number will be examined with particular emphasis on the conditions under which the sidewall boundary layer, of thickness $O(E^{\frac{1}{4}})$, where E is the Ekman number, can separate from the wall, thereby altering the $O(1)$ dynamics of the flow. The particular parameter regime of interest is when the Rossby number Ro is $O(E^{\frac{1}{2}})$, which is the same as that studied by Walker & Stewartson (1972) for flow around a circular cylinder bounded axially by two infinite plates. In their study it is shown that for $Ro/E^{\frac{1}{2}}$ sufficiently large the boundary layer can separate from the cylinder as the flow decelerates on the downstream side. This is in marked contrast with the constant displacement thickness of the flow for $Ro = 0$, for which the boundary-layer solution can be calculated exactly.

A difficulty with the circular cylindrical geometry is that a singularity develops at the rear stagnation point at a lower value of $Ro/E^{\frac{1}{2}}$ than that for which separation first occurs. In the present study this difficulty is averted by examining a flow within an annular container, driven by differential rotation of the lid. This enables a clearer view to be obtained of the development of flow separation in the $E^{\frac{1}{4}}$ layer. Variations in the flow at the sidewall are induced by a small topography, of height $O(E^{\frac{1}{2}})$, on the base of the container. The effect of such topography on a low Rossby number flow was examined theoretically and experimentally by Boyer (1971) who showed that the flow moving across a long narrow ridge was deflected a distance $O(h/E^{\frac{1}{2}})$ along

the ridge as it crossed the obstruction. These results are extended in Huppert & Stern (1974) to include the effects of sidewalls, although $E^{\frac{1}{4}}$ layers are not considered. The influence of sidewall boundary layers is also neglected by Davey (1978) in his study of the flow in an annular container, identical with that considered here. His results concentrate on three parameter regimes, each of which enables the flow equations to be simplified. He also restricts attention to topographies that are independent of radial distance from the cylinder axis, and, for simplicity, a similar assumption will be made here.

When the $E^{\frac{1}{4}}$ layer is studied in this configuration it is found that once the ratio $Ro/E^{\frac{1}{2}}$ exceeds a critical value the boundary layer develops a singularity at a position where the external flow is decelerating. This singularity is similar to that examined by Goldstein (1948) for a separating flow in a non-rotating fluid. Furthermore, using a condition derived by Buckmaster (1969) for a related problem in magnetohydrodynamics, a reasonable estimate for the critical value of $Ro/E^{\frac{1}{2}}$ can be obtained without the need for detailed study of the boundary-layer flow. Since the equations for the interior flow, away from the boundary layers, are nonlinear when Ro is $O(E^{\frac{1}{2}})$ they must, in general, be solved numerically, and the boundary-layer flow, also obtained numerically, must be matched onto the interior flow. Sufficient resolution is available to demonstrate clearly that the $E^{\frac{1}{4}}$ layer may separate from the wall. This implies that when a low-Rossby-number flow, with $Ro \neq 0$, is calculated proper account should be taken of the finite thickness of the boundary layer, as is usual in a non-rotating fluid. An example of this is given in Page (1982), where the flows in the interior and $E^{\frac{1}{4}}$-layers are calculated together for a small, but finite, value of E. In that case no singularities are encountered in the boundary layer, indicating that the interior flow adjusts under the influence of the $E^{\frac{1}{4}}$ layer flow.

The annular geometry studied here enables comparisons to be made with previous theoretical (Davey 1978) and experimental (Maxworthy 1977) work on this configuration. However, unlike in those investigations, a smooth topography extending fully around the container will be used here to demonstrate that the obstacle need not be localized nor must it have discontinuous slope for separation to occur. If the flow separates for a smooth topography then it would certainly be expected to separate when either of the above features leads to larger velocity gradients in the flow against the wall. The smooth topography also enables better numerical resolution of the phenomenon.

The governing equations for the interior flow in an annular container are derived in §2 and numerical results for this flow are presented in §3. The trends in the interior flow as $Ro/E^{\frac{1}{2}}$ and the topography height vary are examined, and in particular it is shown that reversed-flow regions can occur in the interior flow without boundary-layer separation. The $E^{\frac{1}{4}}$ layer effects are studied in §4, where the governing equations are derived and a necessary condition for viscous separation to occur is calculated. The parameters for which flow separation, whether in the interior flow or due to boundary-layer effects, are also given in §4 for a particular form of topography.

2. Formulation

The flows considered are those of an incompressible fluid, of constant density ρ^* and kinematic viscosity ν^*, contained in an annulus, rotating at a uniform angular velocity Ω^*. The inner radius of the container is l^*, the outer radius $bl^*(b > 1)$ and the average depth dl^*. On the base there is a topographical feature of small height h^*, varying in the azimuthal direction but independent of the radial distance from the cylinder axis. Motion in the fluid, relative to a frame rotating with the container,

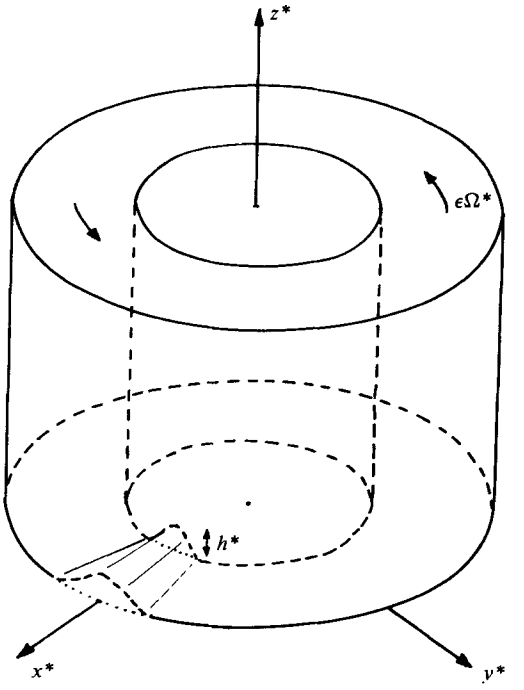

FIGURE 1. The geometrical configuration relative to a frame rotating with angular velocity Ω^*; the fluid is contained in the annular cylinder with radii l^*, bl^* and forced over the topography h^* by differential rotation of the lid.

is forced by rotating the lid with an excess angular velocity $\epsilon\Omega^*$. This configuration is illustrated in figure 1.

The Ekman number E, based on the lengthscale l^*, is defined as

$$E = \frac{\nu^*}{\Omega^* l^{*2}} \ll 1, \tag{2.1}$$

and the Rossby number Ro is

$$Ro = \frac{U^*}{\Omega^* l^*}, \tag{2.2}$$

where $U^* = \epsilon l^* \Omega^*$ is a typical velocity scale. The latter simplifies to $Ro = \epsilon$, which in this study is taken to be $O(E^{\frac{1}{2}})$. The bottom topography, when scaled by l^*, is

$$h = \frac{h^*}{l^*}, \tag{2.3}$$

and this is also considered to be $O(E^{\frac{1}{2}})$.

The non-dimensional coordinates, velocities and time defined in a Cartesian frame are given by

$$\mathbf{x} = \mathbf{x}^*/l^*, \quad \mathbf{u} = \mathbf{u}^*/U^*, \quad t = \Omega^* t^*, \tag{2.4}$$

where $\mathbf{x} = (x, y, z)$ are coordinates measured relative to a frame rotating with the container, and z is aligned with $\hat{\mathbf{k}}$. In terms of these variables the Navier–Stokes equations for a steady flow are

$$Ro(\mathbf{u} \cdot \nabla)\mathbf{u} + 2(\hat{\mathbf{k}} \times \mathbf{u}) = -\nabla P + E\nabla^2 \mathbf{u}, \tag{2.5}$$

$$\nabla \cdot \mathbf{u} = 0, \tag{2.6}$$

where P is the reduced pressure

$$P^* = p^* - \tfrac{1}{2}\rho^*\Omega^{*2}(\mathbf{x}^* \times \hat{\mathbf{k}})^2, \tag{2.7}$$

scaled by $\rho^*\Omega^*U^*l^*$. The boundary conditions on the motion are

$$\mathbf{u} = \mathbf{0} \quad \text{on} \quad r = 1, b \quad \text{and} \quad z = h(\theta), \tag{2.8}$$

$$\mathbf{u} = r\hat{\boldsymbol{\theta}} \quad \text{on} \quad z = d, \tag{2.9}$$

where (r, θ, z) are cylindrical polar coordinates.

For $E \ll 1$ the solution of (2.5) can be expanded in powers of $E^{\frac{1}{2}}$, and the leading-order terms must then satisfy

$$2(\hat{\mathbf{k}} \times \mathbf{u}_0) = -\nabla P_0, \tag{2.10}$$

so the flow, to this order, follows lines of constant pressure. A further consequence of (2.10) is that P_0, and hence $\mathbf{u}_0$, is depth-independent. Therefore a stream function $\psi(r, \theta)$ can be defined from which the horizontal velocity components in polar coordinates

$$u_0 = -\frac{1}{r}\frac{\partial \psi}{\partial \theta}, \quad v_0 = \frac{\partial \psi}{\partial r} \tag{2.11}$$

can be calculated. To determine ψ it is necessary to consider higher-order terms in (2.5), and this is most easily done by eliminating P from the (x, y)-components of (2.5). The resulting equation for the z-component of the vorticity,

$$\zeta = \nabla_1^2 \psi, \tag{2.12}$$

where ∇_1^2 is the two-dimensional Laplacian, is, to lowest order,

$$\frac{Ro}{E^{\frac{1}{2}}} J(\psi, \zeta) = 2\frac{\partial w_1}{\partial z}, \tag{2.13}$$

where J is the two-dimensional Jacobian and, since w is zero to leading order, we have written $w = E^{\frac{1}{2}}w_1 + O(E)$. To determine w_1 the Ekman layers at $z = h, d$ must be considered, and an analysis of these leads to the compatibility conditions (Greenspan 1968)

$$w_1 = \tfrac{1}{2}(2 - \zeta) \quad \text{on} \quad z = d, \tag{2.14}$$

$$w_1 = \tfrac{1}{2}\zeta + J\left(\psi, \frac{h}{E^{\frac{1}{2}}}\right) \quad \text{on} \quad z = h. \tag{2.15}$$

Since ψ, ζ depend on (r, θ) only $\partial w_1/\partial z$ is independent of z, from (2.13), and can be evaluated from (2.14), (2.15) as

$$\frac{\partial w_1}{\partial z} = \frac{1}{d}\left[1 - \zeta - J\left(\psi, \frac{h}{E^{\frac{1}{2}}}\right)\right], \tag{2.16}$$

to lowest order. Substituting this into (2.13) gives

$$J(\psi, \lambda\zeta + h/E^{\frac{1}{2}}) = 1 - \zeta, \tag{2.17}$$

where

$$\lambda = \frac{Ro\, d}{2E^{\frac{1}{2}}}, \tag{2.18}$$

which is a quantity of order unity since Ro is $O(E^{\frac{1}{2}})$. The solution of (2.12) and (2.17) will be known as the interior flow, and the boundary conditions are

$$\psi(1, \theta) = 0, \quad \psi(b, \theta) = Q, \tag{2.19}$$

where Q is an undetermined constant. The indeterminateness arises because, for a given value of ζ, an arbitrary multiple of

$$\psi_{\mathrm{H}} = \ln r \tag{2.20}$$

can be added to a solution of (2.12). This non-uniqueness can be resolved by considering $O(E^{\frac{1}{2}})$ terms in the flow, as done by Davey (1978), leading to the condition

$$\int_0^{2\pi} v_0(1,\theta)\,d\theta = \pi, \tag{2.21}$$

which fixes the value of Q.

A second parameter of interest in this study, where $h = h(\theta)$ is $O(E^{\frac{1}{2}})$, is

$$\alpha = E^{-\frac{1}{2}} \max_{\theta} \left|\frac{dh}{d\theta}\right|, \tag{2.22}$$

which measures the relative importance of the topographic term in (2.17).

3. Interior-flow results

The interior-flow problem has been studied previously by Davey (1978), where three parameter regimes, for which (2.17) can be simplified, were examined in detail. Firstly, when $\alpha \ll (1+\lambda^2)^{\frac{1}{2}}$ the flow is a small perturbation upon the axisymmetric flow $v_0 = \frac{1}{2}r$ and the vorticity equation can be linearized. Secondly, for $\lambda = 0$ the problem is linear and ζ is given explicitly in terms of ψ. Finally, for $\lambda \gg 1$ and $\alpha = O(\lambda)$ the right-hand side of (2.17) is relatively small so that $\lambda\zeta + h/E^{\frac{1}{2}}$ is approximately constant along streamlines. These three regimes do not, however, cover all possible values of (λ, α) and they have the disadvantage of being disjoint so that trends in λ or α are not easy to establish.

Exact solutions are difficult to obtain, even in Davey's simplified regimes, so a full numerical method has been sought that could be used uniformly for $O(1)$ values of λ and α. The numerical scheme is iterative with an alternating-direction iteration used to solve (2.17) at each step. Having found ζ for that step the stream function was calculated by solving (2.12), subject to (2.19) and (2.21), and the whole process was repeated until the solution had converged.

For reasons outlined earlier a simple, smooth topography is used in this study, namely

$$h = \alpha E^{\frac{1}{2}} \sin\theta. \tag{3.1}$$

Numerical solutions were calculated with this form of h, for a wide range of α and λ, using centred finite differences with 40 radial grid points and 64 azimuthal points. These solutions converge to 0·1 % accuracy in 10–20 iterations and are not affected significantly by increasing the number of grid points. Further details are given in Page (1981).

Before examining the boundary-layer flow, which is the main purpose of this paper, some general trends in the interior flow will be outlined. These show why boundary-layer separation can occur and aid in determining when it can be expected.

In figure 2 the flow for zero Rossby number, $b = 2$ and various values of α is illustrated, showing the displacement of the streamlines as the height of the topography is increased; for an observer moving with the flow this displacement is to the left as the fluid moves uphill and to the right as it moves downhill. This is consistent with the theory of Huppert & Stern (1974) and the flows shown in Davey (1978). A consequence of this property is that the slip velocity on each wall has a

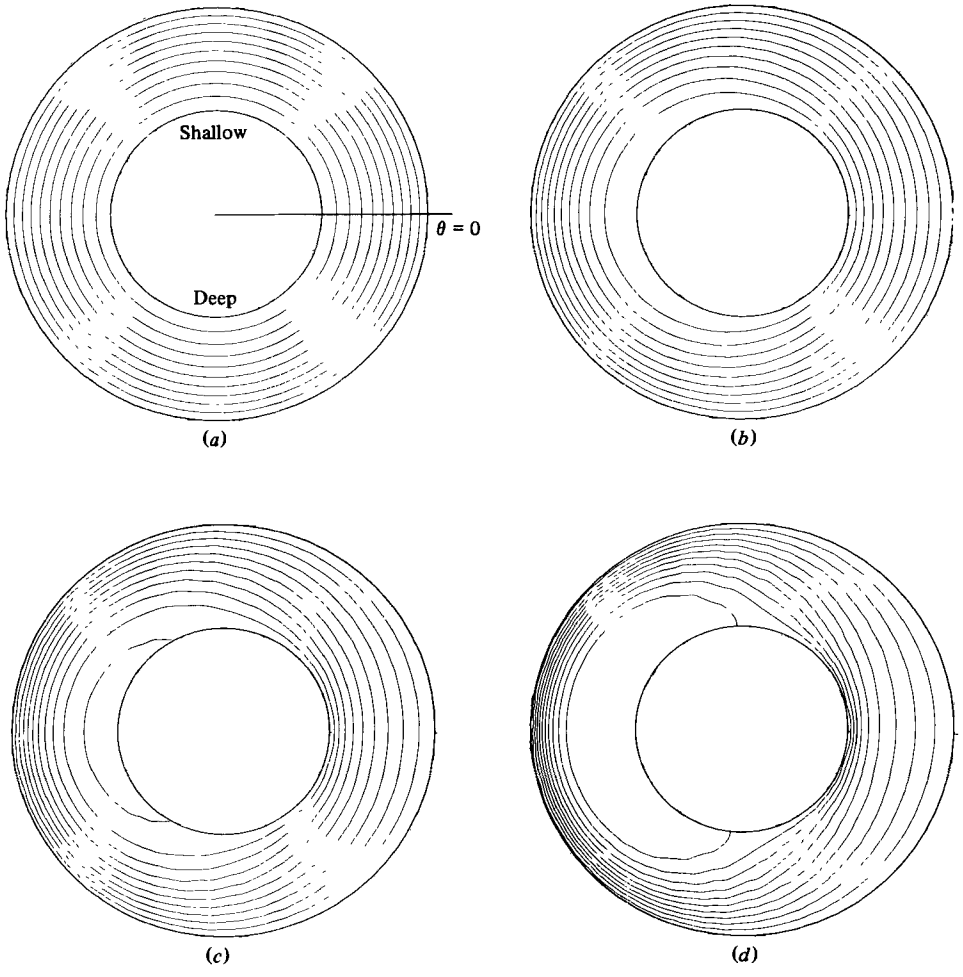

FIGURE 2. Streamline plots for the flow when $Ro = 0$, $b = 2$ and with the topography (3.1) for (*a*) $\alpha = 0$, (*b*) 2, (*c*) 4, (*d*) 8.

variation, about its mean value $\frac{1}{2}$ or $\frac{1}{2}b$, which increases with α. As a result the velocity gradient $r^{-1}\,\partial v_0/\partial\theta$ also increases with α. This is demonstrated in figure 3, where the velocity against the inner wall is plotted for each of the flows in figure 2. These figures also show that for α larger than a critical value, between 2 and 4, there is a region of flow reversal in the interior. This separation of the flow from the wall is not due to viscous effects in the sidewalls since these are not included in this solution. Similar reversed-flow regions are also shown in Davey (1978) for a slightly different topography.

Keeping the height of the topography fixed, at $\alpha = 2$, and increasing λ results in the variation of slip velocities at each wall, as shown in figure 4. The positions of the velocity extrema are displaced downstream by an amount that increases with λ, and as this occurs the magnitude of the velocity variation decreases. In fact for $\alpha = O(1)$ and $\lambda \gg 1$ an asymptotic solution of (2.17) can be calculated, when h is given by (3.1), since

$$\zeta = 1 - \alpha\lambda^{-1}\sin\theta + O(\lambda^{-2}) \tag{3.2}$$

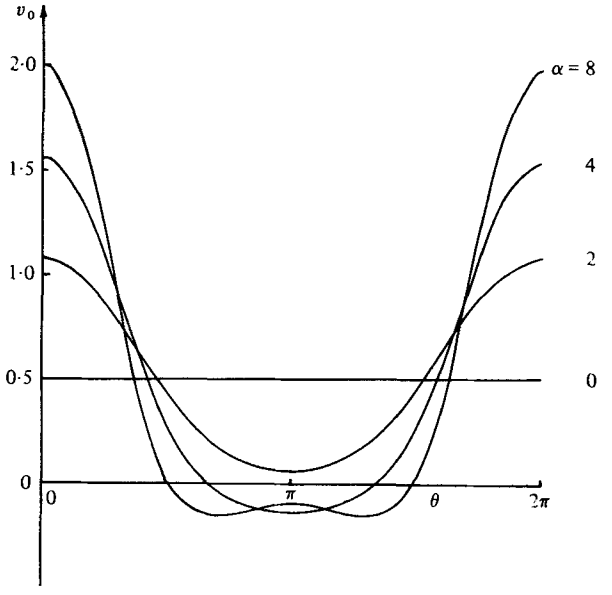

FIGURE 3. Interior-flow velocities against the inner wall, $r = 1$, for each plot shown in figure 2.

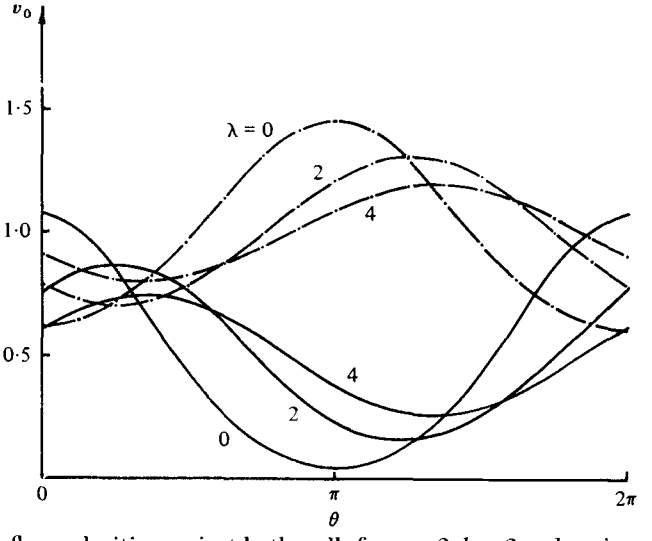

FIGURE 4. Interior-flow velocities against both walls for $\alpha = 2$, $b = 2$ and various values of λ: ——, inner wall; – · –, outer wall.

in that case. This can be solved easily to give the velocity variations on the inner wall as

$$v_0(1, \theta) = \frac{1}{2} + \frac{\alpha(2b+1)(b-1)}{3\lambda(b+1)} \sin\theta. \tag{3.3}$$

Therefore as $\lambda \to \infty$ the velocity variations are $O(\lambda^{-1})$ and the position of the extrema coincide with those of h, a change in azimuth of $\frac{1}{2}\pi$ from the positions of the extrema for $\lambda = 0$ which were at the maxima of $|dh/d\theta|$. Another important feature shown in figure 4 is that the maximum value of $\partial v_0/\partial\theta$ is slightly larger on the inner wall than

on the outer and therefore the velocity gradient $r^{-1}\,\partial v_0/\partial\theta$ is significantly larger for $r = 1$ than for $r = b$.

4. Boundary-layer flow

The interior flow developed in §2 is required to satisfy $u = 0$ on $r = 1, b$ but it will not, in general, satisfy the no-slip condition $v = 0$ on both walls, as required by (2.8). For rotating fluid with zero Rossby number the tangential velocity adjusts to this value across a thin boundary layer of thickness $O(E^{\frac{1}{4}})$ (Stewartson 1957) and a simple exact solution is available for the flow in this layer. From this solution it is apparent that for $Ro = 0$ the boundary layer has no $O(1)$ influence on the interior flow, since the displacement thickness is constant at $\delta = (\frac{1}{2}dE^{\frac{1}{2}})^{\frac{1}{2}}$. Stewartson also examines a thinner layer of thickness $O(E^{\frac{1}{3}})$, across which the vertical velocity adjusts to $w = 0$, but in this study the effect of this layer will be neglected. This can be justified because the velocities in the $E^{\frac{1}{3}}$ layer are small.

Walker & Stewartson (1972, 1974) examine the $E^{\frac{1}{4}}$ layer for non-zero Rossby numbers of $O(E^{\frac{1}{2}})$ in a rotating flow comparable to that studied here, and conclude that for $Ro/E^{\frac{1}{2}}$ larger than a critical value the boundary layer can separate from the wall, thereby leading to a modification of the interior flow. In their study Walker & Stewartson refer to an equivalent problem in magnetohydrodynamics (Leibovich 1967; Buckmaster 1969, 1971) for which a necessary condition for separation to occur was derived. With the notation of §3 this condition is

$$\frac{\lambda}{r}\frac{\partial v_0}{\partial\theta}(r,\theta)+1 \leqslant 0, \tag{4.1}$$

where $r = 1$ or $r = b$, and v_0 is the velocity of the interior flow tangential to the wall. A derivation of (4.1) will be outlined below, once the governing equations for the flow in the $E^{\frac{1}{4}}$ layer have been derived.

The results presented in §3 indicate that, for the topography given by (3.1), the velocity gradients are larger on the inner wall, and therefore the condition (4.1) is satisfied on the inner wall at a smaller value of λ than on the outer wall. Hence, it is sufficient to examine only the boundary layer on $r = 1$.

In this layer $r-1$ is $O(\delta)$, the tangential velocity is $O(1)$ and the vorticity ζ is $O(\delta^{-1})$. As in the interior flow, the geostrophic equation (2.9) is satisfied to lowest order and therefore a scaled stream function $\bar{\psi}(\bar{r}, \theta)$ can be defined in terms of $\bar{r} = (r-1)/\delta$ such that

$$\bar{u} = -\frac{\partial\bar{\psi}}{\partial\theta}, \quad v = \frac{\partial\bar{\psi}}{\partial r}. \tag{4.2}$$

The vorticity to lowest order is, from (2.12),

$$\zeta = \frac{1}{\delta}\frac{\partial\bar{v}}{\partial\bar{r}}, \tag{4.3}$$

and, from (2.5), (2.14), (2.15) and (4.2), it is governed by the equation

$$\lambda\left[\bar{u}\frac{\partial\zeta}{\partial\bar{r}}+\bar{v}\frac{\partial\zeta}{\partial\theta}\right] = -\zeta+\frac{\partial^2\zeta}{\partial\bar{r}^2}. \tag{4.4}$$

This equation can be integrated once to give

$$\lambda\left[\bar{u}\frac{\partial\bar{v}}{\partial\bar{r}}+\bar{v}\frac{\partial\bar{v}}{\partial\theta}\right] = \lambda\bar{v}_{\mathrm{e}}\frac{d\bar{v}_{\mathrm{e}}}{d\theta}+\bar{v}_{\mathrm{e}}-\bar{v}+\frac{\partial^2\bar{v}}{\partial\bar{r}^2}, \tag{4.5}$$

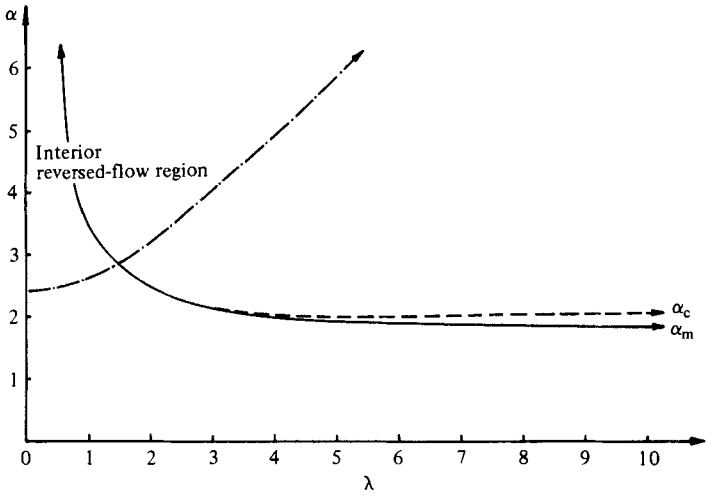

FIGURE 5. Plot of (λ, α) parameter space for $b = 2$ showing the parameters for which interior reversed flow occurs, bounded by —·—, and the values of α_m, α_c.

which, apart from the term $\bar{v}_e - \bar{v}$, is similar to the boundary-layer equation in a non-rotating fluid. The boundary conditions for (4.5) are $\bar{v} \to \bar{v}_e \equiv v_0(1, \theta)$ as $\bar{r} \to \infty$, $\bar{u} = \bar{v} = 0$ on $\bar{r} = 0$, together with a periodicity condition in θ.

The condition (4.1) on a flow with viscous separation follows directly from (4.5) evaluated on $\bar{r} = 0$ since, as in the non-rotating theory, if boundary-layer separation occurs at $\theta = \theta_s$ then $\partial^2 \bar{v}(0, \theta_s)/\partial \bar{r}^2 \geqslant 0$. It follows from the trends in the interior flow, observed in § 3, that for α fixed there is a minimum value of λ at which separation can occur, given by

$$\lambda_m \min_{\theta} \left(\frac{d\bar{v}_e}{d\theta} \right) = -1, \tag{4.6}$$

where $\bar{v}_e$, dependent on the parameters (λ, α), is evaluated at (λ_m, α). Alternatively, there is a minimum topographic height, $\alpha_m(\lambda)$, and this is shown on figure 5, as calculated from the numerical solutions for the interior flow. For $\lambda \gg 1$ and $b = 2$ the asymptotic solution (3.3) implies that $\alpha_m \to 1{\cdot}8$ as $\lambda \to \infty$, in agreement with the numerical solution.

Figure 5 also shows the parameter range for which there is a region of reversed flow in the annulus, due solely to interior flow separation. For λ less than approximately 1·5 reversed flow appears in the interior solution for topography smaller than that for which viscous separation can occur. Therefore for low values of λ flow reversal need not be due to boundary-layer effects. However, for larger values of λ there is the possibility that the flow separates, owing to viscous effects in the $E^{\frac{1}{4}}$ layers, at a lower value of α than that indicated by the interior solutions.

To determine the flow in the boundary layer (4.5) was integrated using the numerical values $v_0(1, \theta)$ from the interior solution. The numerical scheme used was the 'box method' (Keller & Cebeci 1971), as used by Crissali & Walker (1976) for the Walker & Stewartson problem, with a stretched grid containing 70 points in the $\bar{r}$ direction. The marching process was initiated from a minimum of $v_0(1, \theta)$, where the profile could be estimated, and, provided the flow did not separate, it could be shown that the boundary-layer solution was periodic. However, this technique prevents the boundary-layer flow from being calculated when there is reversed flow in the interior,

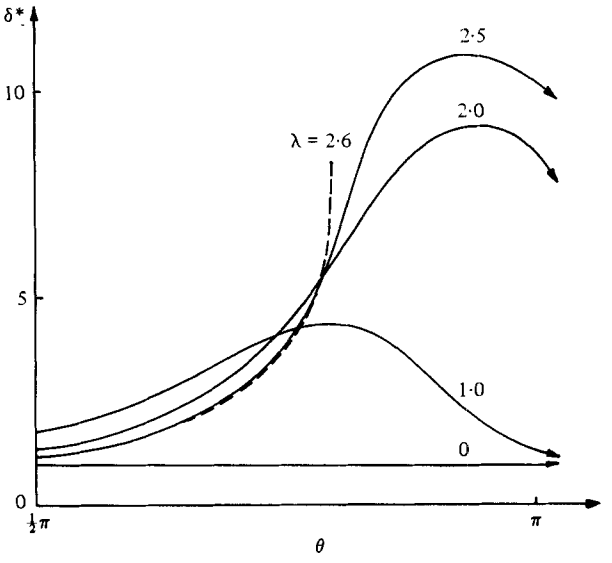

FIGURE 6. The displacement thickness δ^* of the boundary layer on the portion of the wall $\frac{1}{2}\pi \leqslant \theta \leqslant \pi$ when $\alpha = 2{\cdot}2$, $b = 2$ and for various values of λ.

since $\bar{v}_e$ is negative at its minimum. The calculations when no interior reversed flow is present show that once α exceeds a value $\alpha_c \geqslant \alpha_m$ the skin friction vanishes and the $E^{\frac{1}{4}}$ layer solution cannot be continued for $\theta > \theta_s$. Furthermore, since the velocity variations of the interior flow on $r = 1$ increase with α, boundary-layer separation can be expected for all $\alpha > \alpha_c$, including the case where α is large enough for reversed flow to be present in the interior. The values of α_c, calculated by a bisection method, are shown on figure 5, and for λ large they are only slightly larger than α_m. For smaller values of λ, with $\bar{v}_e > 0$ for all θ, the values of α_c and α_m appear to coincide, indicating that $\alpha_c \approx \alpha_m$ in the interior reversed-flow region. If $\alpha > \alpha_c$ in this region then viscous effects can be expected to modify the existing reversed flow.

In figure 6 the displacement thickness δ^* is plotted for α fixed at 2·2, $b = 2$ and increasing values of λ. For $\lambda = 0$ the displacement thickness is $\delta^* = 1$, as expected from the exact solution, but when $\lambda > 0$ the boundary layer thickens as the external flow $\bar{v}_e$ decelerates. For λ between 2·5 and 2·6 the skin friction vanishes in this region, leading to flow separation. However, even for $\lambda = 2{\cdot}5$, when viscous separation has not occurred, the interior solution for any flow with $E \neq 0$ will be affected by the large displacement thickness $\delta^* > 10$ unless the Ekman number is very small.

The results of this study can be compared, at least qualitatively, with the experiments performed by Maxworthy (1977). These flows effectively involve an additional parameter, the obstacle width, but they do consistently show the presence of flow separation. In all of the photographs shown in that paper the values of α, as defined by (2.22), are large and the values of λ, $R_0/E_H^{\frac{1}{2}}$ in his notation, vary from 0·58 to 9·56. Clearly the results presented for the topography (3.1) are not directly applicable to these experiments, although, since the flows show trends with α and λ similar to those observed in §3, the general features are alike. In particular, for the cases where $\lambda > 2$ the maximum streamline displacement, as the flow crosses the obstruction, is close to the point where h is maximum. This property is similar to that observed in Davey's third regime, for α, λ both large, and therefore if the flow

separation in Maxworthy's photographs is not due to viscous effects then the entire flow would be expected to be symmetric. This does not, however, appear to be the case, supporting the argument that the $E^{\frac{1}{4}}$ layer has separated from the inner wall. Therefore care is necessary when comparing the results of these experiments with those from the interior-flow calculations, in which the effects of the sidewall boundary layers are neglected. Moreover, the possibility of $E^{\frac{1}{4}}$ layer separation should be considered in any configuration where the interior flow decelerates on a sidewall and the Rossby number is $O(E^{\frac{1}{2}})$.

The author gratefully acknowledges the assistance provided by Professor L. M. Hocking, who suggested the topic and aided in the development of this paper. The research was completed while the author was at University College London, supported by a Commonwealth Scholarship.

REFERENCES

BOYER, D. L. 1971 Rotating flow over long shallow ridges. *Geophys. Fluid Dyn.* **3**, 165–184.

BUCKMASTER, J. 1969 Separation and magnetohydrodynamics. *J. Fluid Mech.* **42**, 481–498.

BUCKMASTER, J. 1971 Boundary layer structure at a magnetohydrodynamic rear stagnation point. *Q. J. Mech. Appl. Math.* **24**, 373–386.

CRISSALI, A. J. & WALKER, J. D. A. 1976 Nonlinear effects for the Taylor-column for a hemisphere. *Phys. Fluids* **19**, 1661–1668.

DAVEY, M. K. 1978 Recycling flow over bottom topography in a rotating annulus. *J. Fluid Mech.* **87**, 497–520.

GOLDSTEIN, S. 1948 On laminar boundary layer flow near a position of separation. *Q. J. Mech. Appl. Math.* **1**, 43–69.

GREENSPAN, H. P. 1968 *The Theory of Rotating Fluids.* Cambridge University Press.

HUPPERT, H. E. & STERN, M. E. 1974 The effect of side walls on homogeneous rotating flow over two-dimensional obstacles. *J. Fluid Mech.* **62**, 417–436.

KELLER, H. B. & CEBECI, T. 1971 Accurate numerical methods for boundary layer flows. In *Proc. 2nd Int. Conf. on Numerical Methods in Fluid Dynamics* (ed. M. Holt). Lecture Notes in Physics, vol. 8, pp. 92–100, Springer.

LEIBOVICH, S. 1967 Magnetohydrodynamic flow at a rear stagnation point. *J. Fluid Mech.* **29**, 401–413.

MAXWORTHY, T. 1977 Topographic effects in rapidly-rotating fluids: flow over a transverse ridge. *Z. angew. Math. Phys.* **28**, 853–864.

PAGE, M. A. 1981 Rotating fluid flows at low Rossby numbers. Ph.D. thesis, University of London.

PAGE, M. A. 1982 A numerical study of detached shear layers in a rotating sliced cylinder. *Geophys. Astrophys. Fluid Dyn.* (to appear).

STEWARTSON, K. 1957 On almost rigid rotations. *J. Fluid Mech.* **3**, 17–26.

WALKER, J. D. A. & STEWARTSON, K. 1972 The flow past a circular cylinder in a rotating frame. *Z. angew. Math. Phys.* **23**, 745–752.

WALKER, J. D. A. & STEWARTSON, K. 1974 Separation and the Taylor-column problem for a hemisphere. *J. Fluid Mech.* **66**, 767–789.